Journal of Chromatography, 589 (1992) 307–313
Elsevier Science Publishers B.V., Amsterdam

CHROM. 23 734

Binary buffers for indirect absorption detection in capillary zone electrophoresis

Tiansong Wang and Richard A. Hartwick*

Department of Chemistry, State University of New York at Binghamton, Binghamton, NY 13902 (USA)

(First received May 28th, 1991; revised manuscript received September 11th, 1991)

ABSTRACT

The displacement processes in binary buffers (two acids and one base) were studied theoretically and experimentally. An equation that correlates the concentration change of buffer ingredients in the sample zone with their electrophoretic mobility was derived. According to the equation, when the mobility of a sample is between those of the two buffer components, the sample will mainly displace the species to which its mobility is closest. This displacement is termed mobility-selective displacement. Several binary buffers with different mobilities were studied, and the experimental results agreed semi-quantitatively with the theory.

INTRODUCTION

The development of improved detection methods in capillary electrophoresis is essential for the continued growth of applications. In principle, capillary zone electrophoresis (CZE) is well suited for direct analyses for compounds such as aliphatic carboxylic acids, amino acids and inorganic acids. However, many of these classes of compounds lack chromophores at useful wavelengths, or have such low molar absorptivities as to prevent reasonable sensitivity by absorption detection. Instead, conductivity detectors [1–7] and amperometric detectors [7–9] have been developed for the CZE of these compounds. The performance of conductivity and amperometric detectors is generally excellent, with detection limits of 10^{-6}–10^{-7} M for carboxylic acids and amino acids. The problems with these detectors are that they are more difficult to fabricate than absorption detectors and are not yet commercially available.

Another strategy for the detection of UV-transparent compounds in CZE is that of indirect fluorescence or indirect absorption detection. To achieve such indirect detection, an ion with either fluorescence or UV absorption properties, which is called the visualization agent, is added to the mobile phase in order to create a high background signal. The analyte ions that have the same sign of charge as the visualization agent are observed from the reduction of the background signal. Indirect fluorescence detection was first introduced to CZE by Kuhr and Yeung [10], and has been applied to the analysis of amino acids, nucleotides, inorganic anions and sugars [10–13]. Impressive detection limits can be achieved, with concentration limits of $2 \cdot 10^{-7}$ M for $H_2PO_4^-$ being reported [12].

Indirect UV detection in CZE was first reported by Hjertén *et al.* [14]. Foret *et al.* [15] presented more details and observed the effect of ion mobility on the peak shape, indicating that high sensitivity could be obtained by selecting visualization agents which have high molar absorptivities and effective mobilities similar to those of sample ions. More recently, indirect UV detection has been applied successfully to the detection of 30 anions separated by CZE [16].

For indirect absorption detection in CZE, the selection of buffers is critical. Currently, most

0021-9673/92/$05.00

indirect absorption and indirect fluorescence detection have been performed with monobuffers (*i.e.*, one acid and one base), because the displacement process in monobuffer is simple. However, monobuffers have several shortcomings: limited pH range because the pH is restricted by the pK of the acid or the base, not ideal for broad mobility ranges of sample ions because the peak shape will be very poor with increasing mobility difference between the sample and visualization agent [15,17] and limited selection in concentration and molar absorptivity of the visualization agent because of the requirements of buffer capacity and linear range of the detector.

It is expected that binary buffers (*i.e.*, two acids and one base) can be used to overcome several of these limitations, but little work has been done on applications of binary buffers [10]. In this paper, a theoretical analysis and experimental study of binary buffer systems are presented. The effects of ion mobility on the displacement and on the peak shape are discussed.

THEORETICAL

In CZE, each ion migrates according to its own mobility under an electric field. The fundamental electrical property that must be satisfied along the path of the capillary is that the electrical current be constant throughout the capillary length. The relationship of current I_i to ion i is [18]

$$I_i = Z_i C_i \mu_i E A F \tag{1}$$

where Z_i is the value of the charge, C_i is the concentration, μ_i is the ion mobility, E is the applied electric field strength, A is the cross-sectional area of solution and F is the Faraday constant. The total current I is

$$I = \sum I_i \tag{2}$$

In Fig. 1, zone B contains only the buffer with anion 1, anion 2 and cation, thus

$$I_b = (Z_1 C_1 \mu_1 + Z_2 C_2 \mu_2 + Z_+ C_+ \mu_+) E_b A F \tag{3}$$

Zone S contains buffer and sample anion 3 and they share the same cation; the concentration of anion 1 and anion 2 will be different from that in zone B, hence

$$I_s = (Z_1 C_1' \mu_1 + Z_2 C_2' \mu_2 + Z_3 C_3 \mu_3 + Z_+ C_+' \mu_+) E_s A F \tag{4}$$

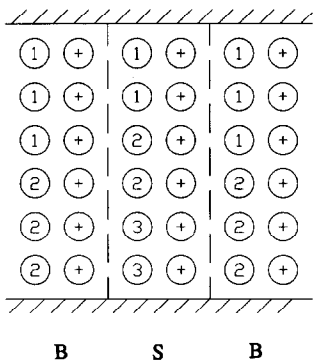

Fig. 1. Representation of two zones in CZE. S, sample zone; B, buffer zone. 1 = Buffer anion 1; 2 = buffer anion 2; 3 = sample anion; + = cation.

It is obvious that $I_s = I_b$, and provided that $C_3 \ll C_1 + C_2$, it is assumed that

$$E_s = E_b \tag{5}$$

Therefore,

$$Z_1 C_1 \mu_1 + Z_2 C_2 \mu_2 + Z_+ C_+ \mu_+ = Z_1 C_1' \mu_1 + Z_2 C_2' \mu_2 + Z_3 C_3 \mu_3 + Z_+ C_+' \mu_+ \tag{6}$$

Let $\Delta C_i = C_i - C_i'$, then eqn. 6 becomes

$$Z_1 \Delta C_1 \mu_1 + Z_2 \Delta C_2 \mu_2 + Z_+ \Delta C_+ \mu_+ = Z_3 C_3 \mu_3 \tag{7}$$

As electroneutrality must hold, then

$$Z_+ C_+ = -(Z_1 C_1 + Z_2 C_2) \tag{8}$$

$$Z_+ C_+' = -(Z_1 C_1' + Z_2 C_2' + Z_3 C_3) \tag{9}$$

Hence

$$Z_+ \Delta C_+ = -(Z_1 \Delta C_1 + Z_2 \Delta C_2 - Z_3 C_3) \tag{10}$$

Combining eqns. 7 and 10, after rearrangement, yields

$$\frac{Z_1 \Delta C_1}{Z_2 \Delta C_2} = \frac{Z_3 C_3 (\mu_3 - \mu_+)}{Z_2 \Delta C_2 (\mu_1 - \mu_+)} - \frac{\mu_2 - \mu_+}{\mu_1 - \mu_+} \tag{11}$$

Assuming that the displacement is in 1:1 ratio in terms of electric charge, then

$$Z_3 C_3 = Z_1 \Delta C_1 + Z_2 \Delta C_2 \tag{12}$$

Combining eqns. 11 and 12, one obtains

$$\frac{Z_1 \Delta C_1}{Z_2 \Delta C_2} = \frac{\mu_3 - \mu_2}{\mu_1 - \mu_3} \tag{13}$$

Eqn. 13 correlates the concentration changes of

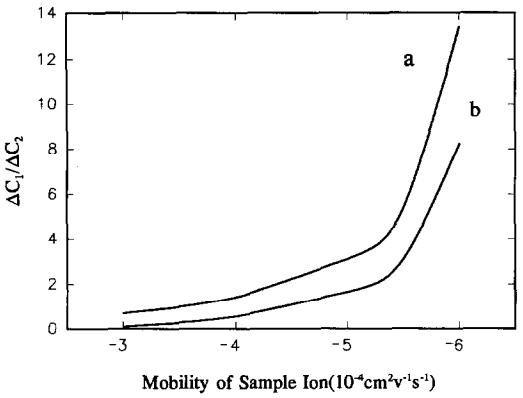

Fig. 2. Relationship between concentration change and ion mobility (eqn. 13). $Z_1 = Z_2 = Z_3$. (a) $\mu_1 = -6.4 \cdot 10^{-4}$, $\mu_2 = -0.64 \cdot 10^{-4}$; (b) $\mu_1 = -6.4 \cdot 10^{-4}$, $\mu_2 = -2.7 \cdot 10^{-4}$.

different buffer components in the sample zone with their mobility and is suitable for Z_1, Z_2 and Z_3 having the same sign and $|\mu_1| > |\mu_3| > |\mu_2|$. This relationship is illustrated in Fig. 2.

EXPERIMENTAL

A Spectra Phoresis 1000 with an SP4400 integrator (Spectra Physics, Reno, NV, USA) was used. The column temperature was 25.0°C, the detector rise time was 0.5 s and sample was injected by a 1.0-s hydrodynamic injection. A laboratory-made PEG bonded capillary and a bare fused-silica capillary (Polymicro Technologies, Phoenix, AZ, USA) were used, both being 75 μm I.D. × 360 μm O.D. with a effective length of 35 cm and a total length 43 cm.

Stock solutions of 10 m*M* 1,3,5-benzenetricarboxylic acids (BTA) and 2 m*M* 1-naphthylacetic acid (NAA) were prepared by dissolving the acids in boiling distilled water. Solutions of lower concentration were obtained by dilution. Buffers of pH 8 were prepared by adding Tris solution.

Sample solutions (malonic acid, tartaric acid, citric acid, propionic acid, hexanoic acid and sodium chloride) of 0.01 *M* were prepared and adjusted to pH 8.0 with Tris solution in order to keep sample pH close to the buffer pH, then diluted to the desired concentration with distilled water. Just before injection, sample solutions were further diluted with buffer in a 1:1 ratio, and the final concentrations were 1.0×10^{-5} *M* for malonic acid and tartaric acid and 2.0×10^{-5} *M* for propionic acid, hexanoic acid and sodium chloride.

The mobilities of BTA and NAA were measured in 1 m*M* phosphate buffer at pH 7.25 and other compounds in 0.5 m*M* BTA–Tris at pH 8.08.

BTA, NAA and hexanoic acid were obtained from Aldrich (Milwaukee, WI, USA), malonic acid and DL-tartaric acid from Sigma (St. Louis, MO, USA), Tris from Bio-Rad Labs. (Richmond, CA, USA) and all other chemicals from Fisher (Fair Lawn, NJ, USA).

RESULTS AND DISCUSSION

One-visualization-agent binary buffer

In this kind of buffer system, the pH is controlled by a secondary non-UV-absorbing component. Hence the disassociation constant of the visualization agent can varied over a broad range, and its concentration can be minimized without a decrease in buffer capacity.

When using a one-visualization-agent binary buffer, competitive displacement between the visualization agent and the pH-controlling ingredient is the problem. There are two cases, as follows.

(1) The mobility of the pH-controlling component is close to that of the visualization agent, and the sample mobility is out of the mobility range of the buffer ingredients. In this instance, common competitive displacement (*i.e.*, no obvious discrimination among the ions to be displaced) takes place, and the sensitivity will obviously be reduced. Two such binary buffers (BTA–citric acid and NAA–hexanoic acid, with the mobilities listed in Table I) were studied and the results are tabulated in Table II. When a binary buffer is used, the sensitivity decreases by 83–90% as the result of competitive

TABLE I

ION MOBILITIES

Compound	μ (10^{-4} cm^2 V^{-1} s^{-1})
NAA	−2.55
Hexanoate	−2.68
Propionate	−3.34
Tartrate	−5.63
Malonate	−6.11
Citrate	−6.20
BTA	−6.39
Chloride	−7.40

TABLE II

COMPARISON OF UNIFORMED PEAK AREA IN MONOBUFFER WITH THAT IN BINARY BUFFER WITH CLOSE MOBILITIES OF BOTH COMPONENTS

Compound	Uniformed peak area (10^3)[a]			
	0.5 m*M* BTA	1.0 m*M* CA[b]–0.1 m*M* BTA	0.3 m*M* NAA	1.0 m*M* HA[c]–0.1 m*M* NAA
Chloride	2.72	0.34	4.13	0.59
Malonate	2.06	–	4.00	0.32
Tartrate	2.15	0.29	3.38	0.38
Propionate	1.30	0.23	4.39	0.56

[a] Uniformed peak area = area/counts retention time.
[b] Citric acid.
[c] Hexanoic acid.

displacement, whereas the noise is reduced only by about 30%. Therefore, this type of binary buffer is generally poor.

(2) The mobility of the pH-controlling component is very different from that of the visualization agent and the sample mobility is in the mobility range of the buffer components. In this instance, mobility-selective displacement will take place. According to eqn. 13, the sample will mainly displace the species to which its mobility is closest, and this process is independent of the concentration of both buffer ingredients. For instance, using BTA–hexanoic acid binary buffer, $\mu_1 = -6.39 \times 10^{-4}$ (BTA), $\mu_2 = -2.68 \times 10^{-4}$ (hexanoate), and when the sample mobility is -6.11×10^{-4} (malonic acid), the concentration change of BTA will be 12.2 times that of hexanoic acid. In other words, the decrease in sensitivity is only 7.6%. The experimental results are given in Table III. Using 1.5 m*M* hexanoic acid–0.5 m*M* BTA binary buffer, the uniformed peak areas of malonate and tartrate are not much different from those in 0.5 m*M* BTA monobuffer, and the uniformed peak areas of these two compounds in 1.5 m*M* hexanoic acid–0.05 m*M* BTA binary buffer are even slightly higher than those in 0.5 m*M* BTA monobuffer, which may be caused by the variation of injection and by the reduction of noise. Generally, the data in Table III are in semi-quantitative agreement with eqn. 13, in that the competitive displacement of hexanoate is supressed in the zones of malonate and tartrate which have mobilities close to that of BTA, and this situation is obviously not affected by the concentration ratio of the pH-controlling component to the visualization agent in the range 3:1–30:1.

TABLE III

COMPARISON OF UNIFORMED PEAK AREA IN MONOBUFFER WITH THAT IN BINARY BUFFER WITH VERY DIFFERENT MOBILITIES OF BOTH COMPONENTS

Compound	Uniformed peak area (10^3)[a]		
	0.5 m*M* BTA	1.5 m*M* HA[b]–0.5 m*M* BTA	1.5 m*M* HA[b]–0.05 m*M* BTA
Chloride	2.72	1.40	1.06
Malonate	2.06	1.83	2.68
Tartrate	2.15	2.19	2.78
Propionate	1.30	no peak	no peak

[a] Uniformed peak area = area/counts retention time.
[b] Hexanoic acid.

When the sample mobility is out of the mobility range of the buffer components, common competitive displacement will dominate again; the higher the concentration of non-UV-absorbing ions, the greater is the decrease in sensitivity, as indicated by chloride in Table III.

Other evidence of mobility-selective displacement is provided by the peak shape. Fig. 3 presents two electropherograms, one obtained from 1.0 m*M* hexanoic acid–0.1 m*M* NAA buffer and the other from 1.5 m*M* hexanoic acid–0.05 m*M* BTA buffer. Although both buffers contain the same pH-con-

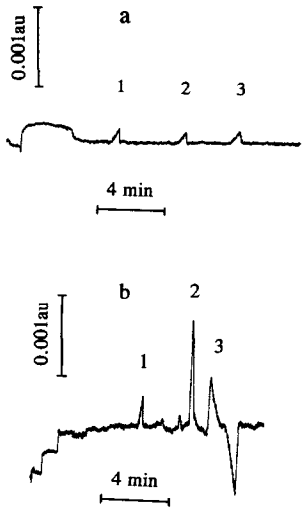

Fig. 3. Comparison of peak shape in one-visualization-agent binary buffers. (a) 1.0 m*M* hexanoic acid – 0.1 m*M* NAA–Tris (pH 8.08); (b) 1.5 m*M* hexanoic acid–0.05 m*M* BTA–Tris (pH 8.09). PEG bonded capillary. Peaks: 1 = chloride; 2 = malonate; 3 = tartrate ($1 \cdot 10^{-5}$–$2 \cdot 10^{-5}$ *M* each).

trolling component, the peak shape is very different. In hexanoic acid–NAA buffer, all peaks are obviously fronting, because the sample ions have much higher mobilities than either hexanoate or NAA. If common competitive displacement was dominant, the replacement of a small amount of NAA with BTA would obviously not affect the peak shape. However, in hexanoic acid–BTA buffer, the peak of malonate becomes symmetrical and the peak of tartrate changes to tailing, similarly to those in BTA monobuffer. Therefore, it is believed that the displacement takes place mainly between BTA and sample (malonate and tartrate), the effect of hexanoate being supressed.

Two-visualization-agent binary buffer

Because of the mobility-selective displacement in binary buffer, the peak shape can be controlled by either of the buffer components. When a buffer is prepared from two visualization agents with different mobilities, good peak shape for ions over a broad mobility range is expected. The experimental results using such a binary buffer can be seen from Table IV and Fig. 4. In BTA monobuffer, the fast ion (malonate) yields a good peak, whereas the slow ion (hexanoate) gives a poor peak. In NAA monobuffer, the situation reversed, *i.e.*, the fast ion generates a poor peak whereas the slow ion generates a good peak. When using BTA–NAA binary buffer, poor peaks seem to disappear and only the good peaks remain. For tartrate, there is no improvement in peak shape, because its mobility is not close enough to that of any visualization agent. In order to improve the peak shape of tartrate, a third visualization agent may be necessary. From this general behavior, it is evident that multi-visualization agents with small (or, ideally, continuous) mobility intervals will be ideal for analyses for ions with broad mobility ranges.

Disturbance peak in binary buffer

In the analysis using BTA–hexanoic acid buffer, a positive peak always appears (Fig. 3b), and peaks with retention times longer than the positive peak disappear, such as propionic acid (Table III). The retention time of the positive peak varies with the concentration ratio of the two buffer components.

TABLE IV

COMPARISON OF PEAK SHAPE AND EFFICIENCY IN MONOBUFFER WITH THOSE IN BINARY BUFFER

Compound	0.3 m*M* BTA		1.0 m*M* NAA		0.25 m*M* BTA–0.25 m*M* NAA	
	N (10^4)[a]	b/a[b]	N (10^4)	b/a	N (10^4)	b/a
Hexanate	4.56	0.29	7.75	0.76	8.06	1.2
Tartrate	3.74	0.18	2.41	7.8	3.02	0.16
Malonate	4.43	0.56	1.37	12	4.10	0.50

[a] Theoretical plate number measured at half-height.
[b] Asymmetry factor measured at 10% of peak height.

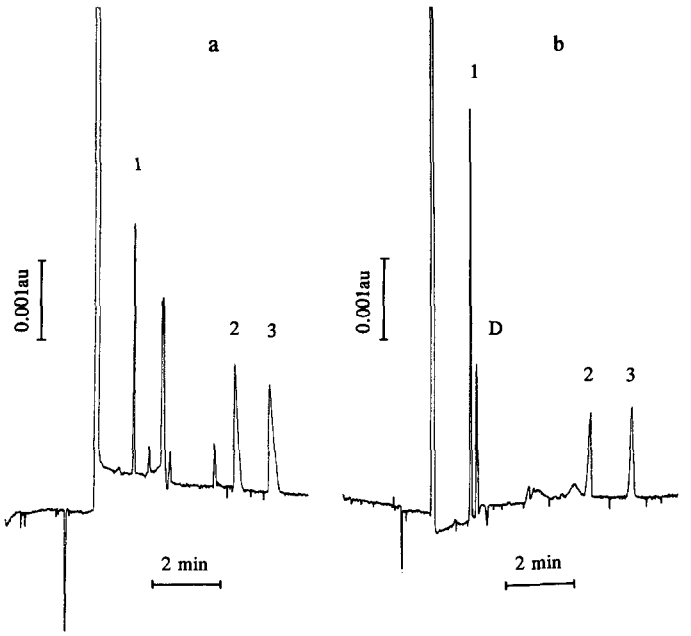

Fig. 4. Comparison of peak shape in monobuffer and in binary buffer. (a) 1.0 m*M* NAA–Tris (pH 8.09); (b) 0.25 m*M* NAA–0.25 m*M* BTA–Tris (pH 8.09). Bare fused-silica capillary. Peaks: 1 = hexanoate; 2 = tartrate; 3 = malonate; D = disturbance peak.

In two-visualization-agent binary buffer, a disturbance peak is also found, but is of negative response. This disturbance peak causes the disappearance of the acetate peak. At present, the disturbance peak is an unsolved problem.

CONCLUSIONS

In binary buffers, there are two kinds of displacement: common competitive displacement which causes a severe decrease in sensitivity, and mobility-selective displacement, which does not lead to obvious decreases in sensitivity. The dominant displacement depends on the mobilities of each species. Theoretical analysis (eqn. 13) indicates that, when the mobility of a sample ion lies between the mobilities of the two buffer components, the sample will mainly displace the species to which its mobility is closest. The experimental results for sensitivity and peak shape support this theory.

In mobility-selective displacement, the peak shape depends on the mobility of the buffer component that dominates the displacement. An improvement in peak shape for both fast and slow ions is observed using the two-visualization-agent binary buffer.

ACKNOWLEDGEMENTS

This research was supported by Spectra-Physics Autolab Division and by the Center for Biotechnology at Stonybrook.

REFERENCES

1 F. E. P. Mikkers, F. M. Everaerts and Th. P. E. M. Verheggen, *J. Chromatogr.*, 169 (1979) 11.
2 P. Gebauer, M. Deml, P. Boček and J. Janak, *J. Chromatogr.*, 267 (1983) 455.
3 J. L. Beckers, Th. P. E. M. Verheggen and F. M. Everaerts, *J. Chromatogr.*, 452 (1988) 591.
4 X. Huang, T. J. Pang, M. J. Gordon and R. N. Zare, *Anal. Chem.*, 59 (1987) 2747.
5 X. Huang, J. A. Luckey, M. J. Gordon and R. N. Zare, *Anal. Chem.*, 61 (1989) 766.
6 X. Huang, M. J. Gordon and R. N. Zare, *J. Chromatogr.*, 480 (1989) 285.
7 X. Huang, R. N. Zare, S. Sloss and A. G. Ewing, *Anal. Chem.*, 63 (1991) 189.
8 R. A. Wallingford and A. G. Ewing, *Anal. Chem.*, 60 (1988) 1972.

9 T. M. Olefirowicz and A. G. Ewing, *J. Chromatogr.*, 499 (1990) 713.
10 W. G. Kuhr and E. S. Yeung, *Anal. Chem.*, 60 (1988) 1832.
11 W. G. Kuhr and E. S. Yeung, *Anal. Chem.*, 60 (1988) 2642.
12 L. Gross and E. S. Yeung, *J. Chromatogr.*, 480 (1989) 169.
13 T. M. Garner and E. S. Yeung, *J. Chromatogr.*, 515 (1990) 639.
14 S. Hjertén, K. Elenbring, F. Kilar, J. L. Liao, A. J. C. Chen, C. J. Siebert and M. D. Zhu, *J. Chromatogr.*, 403 (1987) 47.
15 F. Foret, S. Fanali, L. Ossicini and P. Boček, *J. Chromatogr.*, 470 (1989) 299.
16 W. R. Jones, P. Jandik and R. Pfeifer, *Am. Lab.*, 23, No. 8 (1991) 40.
17 F. E. P. Mikkers, F. M. Everaerts and Th. P. E. M. Verheggen, *J. Chromatogr.*, 169 (1979) 1.
18 P. W. Atkins, *Physical Chemistry*, W. H. Freeman, New York, 4th ed., 1990, p. 756.